Biochimica et Biophysica Acta 1838 (2014) 2625–2634

Contents lists available at ScienceDirect

Biochimica et Biophysica Acta

journal homepage: www.elsevier.com/locate/bbamem

Self-assembly and interactions of short antimicrobial cationic lipopeptides with membrane lipids: ITC, FTIR and molecular dynamics studies

Emilia Sikorska [a,*], Małgorzata Dawgul [b], Katarzyna Greber [b], Emilia Iłowska [a], Aneta Pogorzelska [b], Wojciech Kamysz [b]

[a] Faculty of Chemistry, University of Gdańsk, Wita Stwosza 63, 80-308 Gdańsk, Poland
[b] Faculty of Pharmacy with Subfaculty of Laboratory Medicine, Medical University of Gdańsk, Al. Gen. J. Hallera 107, 80-416 Gdańsk, Poland

ARTICLE INFO

Article history:
Received 13 February 2014
Received in revised form 13 May 2014
Accepted 23 June 2014
Available online 28 June 2014

Keywords:
Lipopeptide
Surfactant-like peptide
Self-assembling process
FTIR
ITC
Coarse-grained molecular dynamics

ABSTRACT

In this work, the self-organization and the behavior of the surfactant-like peptides in the presence of biological membrane models were studied. The studies were focused on synthetic palmitic acid-containing lipopeptides, C_{16}–KK–NH_2 (**I**), C_{16}–KGK–NH_2 (**II**) and C_{16}–KKKK–NH_2 (**III**). The self-assembly was explored by molecular dynamics simulations using a coarse-grained force field. The critical micellar concentration was estimated by the surface tension measurements. The thermodynamics of the peptides binding to the anionic and zwitterionic lipids were established using isothermal titration calorimetry (ITC). The influence of the peptides on the lipid acyl chain ordering was determined using FTIR spectroscopy. The compounds studied show surface-active properties with a distinct CMC over the millimolar range. An increase in the steric and electrostatic repulsion between polar head groups shifts the CMC toward higher values and reduces the aggregation number. An analysis of the peptide–membrane binding revealed a unique interplay between the initial electrostatic and the subsequent hydrophobic interactions enabling the lipopeptides to interact with the lipid bilayer. In the case of C_{16}–KKKK–NH_2 (**III**), compensation of the electrostatic and hydrophobic interactions upon binding to the anionic membrane has been suggested and consequently no overall binding effects were noticed in ITC thermograms and FTIR spectra.

1. Introduction

The rapid emergency of bacterial resistance to conventional antibiotics puts an increased challenge in the search of alternative treatment strategies. Infection caused by resistant microorganisms failing to respond to conventional treatment, results often in prolonged illness, greater risk of death and higher costs. Antimicrobial peptides (AMPs) are one of the most promising classes of compounds with potential use in antibiotic therapy. They are gene-encoded peptides being part of the innate immune system to the microbial invasion of microorganisms of all types [1]. A specific structural feature of the majority of antibacterial peptides is the presence of strongly basic amino acid residues (Lys, Arg) providing a net positive charge ranging from +2 to +9. This feature is undoubtedly important for initial electrostatic attraction between AMPs and negatively charged membranes of bacteria or other microorganisms, which leads to an increase in peptide concentration on the membrane surface. Upon reaching a threshold membrane-bound concentration, a peptide begins to penetrate into the lipid bilayer via a number of possible mechanisms. The most frequently proposed mechanisms of antimicrobial peptide–membrane disruption are a carpet mechanism, as well as a barrel-stave pore and a toroidal pore formation [2,3]. This leads to uncontrolled efflux of essential ions and nutrients and ultimately to death of the bacterial cell [4–8]. The incredible advantages of antimicrobial peptides are their broad-spectrum activity and potentially low levels of induced resistance [9]. However, some disadvantages, such as poor bioavailability and high cost of production need to be overcome [10]. Therefore, numerous studies on peptides have been focused on designing short synthetic analogues exhibiting antimicrobial activity as well as optimization of the synthetic methods. An interesting alternative seems to be short synthetic cationic lipopeptides. Lipopeptides containing positively charged amino acid residues and fatty acid tails have an amphipathic structure, essential features of antibiotic peptides. In addition, the presence of hydrophobic tail and hydrophilic head determines surface-active properties of short lipopeptides. An important advantage of the lipopeptides is their relatively rapid biodegradability

Abbreviations: C_{16}, palmitic acid; CG MD, coarse-grained molecular dynamics; DPPC, 1,2-dipalmitoyl-*sn*-glycero-3-phosphocholine; DPPG, 1,2-dipalmitoyl-*sn*-glycero-3-phosphoglycerol; LUV, large unilamellar vesicle; MLV, multilayer vesicle; POPC, 1-palmitoyl-2-oleoyl-*sn*-glycero-3-phosphocholine; POPG, 1-palmitoyl-2-oleoyl-*sn*-glycero-3-phosphoglycerol

* Corresponding author. Tel.: +48 58 523 50 80; fax: +48 58 523 50 12.
E-mail address: emilia.sikorska@ug.edu.pl (E. Sikorska).

http://dx.doi.org/10.1016/j.bbamem.2014.06.016
0005-2736/

[11], unlike that of conventional surfactants, the feature compatible with the modern trend of developing environmentally friendly chemicals.

In this paper we report on our studies on the activity, self-organization and interactions of three short synthetic *N*-terminal palmitoylated peptides: C_{16}–KK–NH_2 (**I**), C_{16}–KGK–NH_2 (**II**) and C_{16}–KKKK–NH_2 (**III**) (Fig. 1) with models of biological membranes. An antistaphylococcal activity of the lipopeptides was earlier reported by Dawgul et al. [12]. Those studies revealed also a high effectiveness of C_{16}–KK–NH_2 (**I**) against biofilms formed by clinical *Staphylococcus aureus* isolates [10] and its ability to enhance the effect of vancomycin in the in vivo study on the prevention of vascular graft staphylococcal infections [13]. In the present work, the activity assays of all the lipopeptides against *S. aureus* were repeated and supplemented by activity assays against other representative Gram-positive and Gram-negative bacteria. Moreover, to explore hemolytic activity of the lipopeptides, they were also tested against a highly diluted solution of human erythrocytes. The thermodynamic parameters for binding of the peptides to the anionic and zwitterionic lipids were established using isothermal titration calorimetry (ITC). The influence of the peptides on the lipid acyl chain ordering was determined using FTIR spectroscopy. Taking into account that the lipopeptides might act as surfactants, the critical micellar concentration was estimated by the surface tension measurements. In addition, molecular dynamics simulations using a coarse-grained force field have also been employed to explore self-assembly, micellar properties and interactions with a model of bacterial membrane.

2. Materials and methods

2.1. Reagents

All the lipopeptides were synthesized manually by solid-phase method on a Polystyrene AM-RAM resin (0.76 mmol/g, Rapp Polymere, Germany) using Fmoc [14] chemistry. Details of the peptide synthesis have been previously described [12]. 1,2-Dipalmitoyl-*sn*-glycero-3-phosphocholine (DPPC), 1,2-dipalmitoyl-*sn*-glycero-3-phosphoglycerol (DPPG), 1-palmitoyl-2-oleoyl-*sn*-glycero-3-phosphocholine (POPC), and 1-palmitoyl-2-oleoyl-*sn*-glycero-3-phosphoglycerol (POPG) were purchased from Sigma-Aldrich.

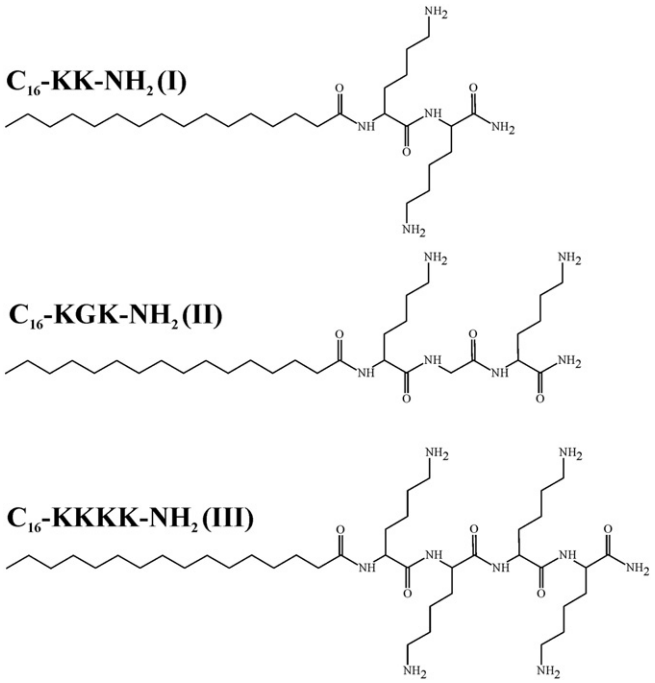

Fig. 1. Chemical structures of experimental compounds.

2.2. Antimicrobial assay

The minimum inhibitory concentration (MIC) and minimum bactericidal concentration (MBC) were determined according to the Clinical Laboratory Standards Institute (CLSI) guidelines. Reference strains of human pathogens were obtained from the Polish Collection of Microorganisms (Polish Academy of Science, Wrocław, Poland). The following strains were tested: *Bacillus subtilis* (ATCC 6633), *Enterococcus faecalis* (ATCC 29212), *Escherichia coli* (ATCC 25922), *Klebsiella pneumoniae* (ATCC 700603), *Pseudomonas aeruginosa* (ATCC 9027) and Staphylococcus *aureus* (ATCC 25923).

MIC was determined by the microbroth dilution method with Mueller-Hinton II liquid medium (Becton Dickinson, France). The tested bacterial strains at an initial inoculum of 5×10^5 CFU/mL were added to polystyrene 96-well plates (Kartell, Italy) and exposed to the lipopeptides at graded concentrations (1–512 μg/mL). After 18 h of incubation at 37 °C the results were read visually, and MIC was recorded as the lowest concentration of a tested compound at which the inhibition growth was clearly visible. For each plate, the positive (microorganisms in liquid media) and negative (sterility) controls were performed.

All the MIC wells which did not show turbidity were cultured on the Mueller-Hinton II Agar. The lowest concentrations of lipopeptides that did not show any visible growth on the plates after 24 h of incubation at 37 °C were taken as the MBCs. The experiments were performed in triplicate on three different days.

2.3. Hemolytic activity

The hemolytic activity of the tested compounds was measured after exposure of human red blood cells to the lipopeptides at graded concentrations (1–128 μg/mL). The compounds were dissolved in DMSO and diluted in phosphate buffer (PBS). The final concentration of DMSO in the sample was 2.5 %. Red blood cells, obtained from a healthy donor were separated from plasma by centrifugation. Then they were washed three times in PBS, centrifuged and resuspended in PBS (final concentration of the red cells per sample was 4% (v/v)). The erythrocytes were incubated with different concentrations of lipopeptides at 37 °C for 1 h and centrifuged (5 min, 1000 *g*). The supernatants were transferred to 96-well plates and hemoglobin release was measured with an Epoch microplate reader (BioTek, USA) by recording the absorbance at 550 nm. A 0.1% Triton X-100 solution was used as a positive control and pure PBS with DMSO (2.5%) as the negative control.

2.4. Preparation of liposomes

For FTIR measurements, multilamellar vesicles (MLVs) consisting of DPPC or DPPG were prepared by dissolving the lipids in a chloroform: methanol (2:1; v/v) mixture at a concentration of 50 mg/mL, evaporated under nitrogen and desiccated under vacuum overnight to remove any residual solvents. The dried films were then resuspended in a 10 mM phosphate buffer, pH 7.4, containing 2.7 mM potassium chloride and 137 mM sodium chloride, with a gentle vortex mixing for 2 h at 45 °C (the temperature above the main phase transition point [15]). In the case of peptide–lipid samples, a lyophilized peptide was blended with the MLV suspension to obtain the desired peptide-to-lipid ratio and the peptide–liposome mixture was incubated for 2 h at 45 °C. In the next step, the samples were frozen and thawed for 5 cycles to reduce the liposome size and lamellarity. A single freeze–thaw cycle consisted of freezing for 5 min at a dry ice temperature (−78 °C) and subsequent thawing for 5 min in a water bath at 45 °C.

In the ITC measurements, POPC or POPG was used as a simple model of membranes. The vesicles made of POPC or POPG (phase transition point, $T_m = -2$ °C) remain in the liquid crystalline phase at room temperature [16]. Therefore, after suspending in phosphate buffer (pH 7.4), the samples with liposomes were vortexed for 2 h at room

temperature. Moreover, for the ITC measurements, large unilamellar vesicles (LUVs) were prepared by extrusion (ten times) of the MLV suspension through polycarbonate membranes (100 nm in diameter, Whatman International Ltd.) using a mini-extruder (Avanti Polar Lipids, Inc.).

2.5. FTIR measurements

The spectra were recorded using a model IFS66 Bruker infrared spectrometer equipped with a DTGS detector (Physicochemical Laboratories, Faculty of Chemistry, University of Gdansk, Poland). Peptide–lipid samples were placed between two CaF_2 windows, which were separated by a 50-μm thick Teflon spacer. The samples were thermostated by a Haake C10 circulator (Gebrüder HAAKE GmbH, Karlsruhe, Germany). Additionally, the temperature of the samples was controlled with a CHY502 thermometer. The samples were examined over the 24–50 °C temperature range. The temperature was equilibrated for 10 min after each step. The spectra were recorded as average of 10 measurements, each with 16 scans and the spectral resolution of 2 cm^{-1}. For data processing, the Bruker OPUS FT-IR software was used. A spectrum of the phosphate buffer (10 mM, pH 7.4) recorded at appropriate temperature was used as the reference and subtracted from the sample spectra. The wavenumber position for the symmetric CH_2 stretching mode was determined using a multiple Gaussian curve fitting procedure (Origin 7 software) in the region between 3000 and 2800 cm^{-1}. Before fitting, the baseline was corrected in the spectral region indicated. A second derivative spectrum was used to determine the position of bands contributing to the spectral interval. The results were plotted against temperature.

2.6. ITC measurements

All ITC experiments were performed at 25 °C using an AutoITC isothermal titration calorimeter (MicroCal Inc., Northampton, USA) with a 1.4491-mL sample and reference cells. The reference cell was filled with distilled water. An initial 2-μL injection was discarded from each dataset in order to remove the effect of titrant diffusion across the syringe tip during the equilibration process. The experiment consisted of injecting 4.1 μL (46 injections, 2 μL for the first injection only) of the liposome solution at a concentration falling in the range of 1.16–1.41 mM into the reaction cell initially containing the buffered (10 mM phosphate buffer, pH 7.4) 0.05 mM peptide solution. A background titration was performed using identical titrant with the buffer solution placed in the sample cell. The result was subtracted from each experimental titration to account for the heat of dilution. All the solutions were degassed before titrations. The titrant was injected at 4-min intervals to ensure that the titration peak returned to the baseline prior to the next injection. Each injection lasted 8 s. To ensure a homogeneous mixing in the cell, the stirring speed was kept constant at 300 rpm.

The stoichiometry (n), association constant (K_a), and change in enthalpy (ΔH) were found by fitting the titration result data to one set of sites model using Origin 7 from MicroCal. Changes in entropy (ΔS) and the Gibbs free energy (ΔG) were calculated from the following equation, wherein factor 55.5 is the molar concentration of water, R is the gas constant (1.986 $cal \cdot mol^{-1} \cdot K^{-1}$) and T is the absolute temperature:

$$\Delta G = -RT \ln(55.5K_a) = \Delta H - T\Delta S.$$

2.7. CMC measurements

The CMC of the lipopeptides was determined by plotting the surface tension against the logarithm of lipopeptide concentration and was found as the intersection of two lines that best fit through the pre- and post-CMC data. Concentrated solutions of individual lipopeptides of known concentration were progressively diluted. All surfactant solutions were prepared in water purified by HLP5 system. The surface tension of each sample was determined at 25 °C by the Du Noüy ring method on an Easy Dyne tensiometer (Krüss GmbH, Germany).

2.8. Molecular dynamics simulations

Simulations were carried out using the GROMACS 4.5.5 package [17]. The MARTINI coarse-grained force field [18,19] was used to model the spontaneous self-organization of C_{16}–KK–NH_2 (**I**), C_{16}–KGK–NH_2 (**II**) and C_{16}–KKKK–NH_2 (**III**) into micelles. To generate the initial configurations, 100 molecules of each lipopeptide were placed at random positions in a cubic box with the edge size of 120 Å. The system was solvated by CG water beads (12,955, 12,744 and 12,158 for **I**, **II** and **III**, respectively), wherein each bead was representative of four real water molecules. The detergent concentration of the micelles during molecular dynamics simulations was ca. 100 mM. As all the lysine side chains were positively charged, CG chloride ions were added to neutralize the entire system. In the next step, the system was energy-minimized before MD simulations, using 10,000 steps of the steepest descent method. Afterwards, the NPT simulations were performed for 1 μs. The time step of 10 fs, as suggested by Wigner et al. [20], was employed during the entire NPT simulations. The temperature was held at 303 K using the Nose–Hoover temperature coupling. The pressure was treated isotropically at 1 bar using the Parrinello–Rahman barostat with a coupling constant $\tau_p = 1.0$ ps and an isothermal compressibility of 4.5×10^{-5} bar^{-1}. The relative dielectric constant for explicit screening was 15. Electrostatics were computed using a shift function with a coulomb cutoff of 12 Å. Shift function was used for van der Waals as well, with a switch distance of 9 Å and a cutoff of 12 Å. The neighbor list was updated every 5 steps using a cutoff r = 14 Å.

To explore lipopeptide–membrane interactions, identical procedure was repeated in the presence of hydrated systems containing phosphatidylethanolamine (POPE) and phosphatidylglycerol (POPG) phospholipid molecules arranged in the bilayer structure. To mimic the membrane of Gram-positive bacteria, a POPE and POPG mixture at a molar ratio of 1:3 was used [21]. The system was built using *insane.py* script available on MARTINI website (http://cgmartini.nl/cgmartini/). A total of 986 lipids were split and equally distributed between two membrane leaflets. One hundred molecules of each lipopeptide were placed randomly on one leaflet of the membrane. The lipid to lipopeptide ratio was ca. 10:1. The entire system was solvated and neutralized by adding sodium and chloride ions. The concentration of free salt ions was ca. 100 mM. Simulations of lipopeptide–membrane interactions were carried out in the isothermal–isobaric (NPT) ensemble with semi-isotropic pressure of 1 bar and at a constant temperature of 303 K. The CG MD simulations for each system were run for 2 μs.

3. Results and discussion

3.1. Biological and hemolytic activities of the lipopeptides

The lipopeptides were assayed against representative Gram-positive and Gram-negative bacteria as well as against a highly diluted solution of human erythrocytes. Results of the microbiological tests are summarized in Table 1, whereas those of hemolytic activity are displayed in Fig. 2. As seen in Table 1, modification of the polar part of the lipopeptide does not affect significantly its antimicrobial activity. The minimum inhibitory concentrations (MICs) of the lipopeptides studied ranged from 4 to 16 μg/mL, while the minimal bactericidal concentrations (MBCs) ranged from 4 to 32 μg/mL. The MBC/MIC ratios are less than or equal 2, asserting the bactericidal power of the tested compounds.

The hemolytic activity studies revealed that C_{16}–KK–NH_2 (**I**) showed the highest hemolytic effectiveness (Fig. 2). In the concentration range of 16–128 μg/mL, a rapid increase in the hemolytic activity was

Table 1
Antimicrobial activity of lipopeptides against representative Gram-positive and Gram-negative bacteria.

Lipopeptide	Gram-positive bacteria			Gram-negative bacteria		
	S. aureus	*B. subtilis*	*E. faecalis*	*E. coli*	*K pneumoniae*	*P. aeruginosa*
Minimum inhibitory concentration [MIC μg/mL]						
C_{16}–KK–NH_2	8	4	8	8	16	8
C_{16}–KGK–NH_2	8	4	8	8	16	16
C_{16}–KKKK–NH_2	4	4	16	8	4	8
Minimum bactericidal concentration [MBC μg/mL]						
C_{16}–KK–NH_2	8	4	8	8	16	8
C_{16}–KGK–NH_2	8	4	16	8	16	32
C_{16}–KKKK–NH_2	8	4	16	8	8	8

observed for this compound, contrary to the remaining ones. At a concentration of ca. 25 mg/mL, C_{16}–KK–NH_2 (**I**) caused the 50% lysis of human erythrocytes, whereas with C_{16}–KKKK–NH_2 (**III**) the concentration required for the 50% lysis was about five times higher (128 mg/mL).

3.2. Calorimetric studies: binding of lipopeptides to lipid vesicles

The binding isotherms were determined by injecting either POPG or POPC lipid vesicles into the peptide solution, i.e. by gradually reducing the free peptide concentration in the reaction cell. On this basis, the enthalpy of binding of the lipopeptide to the liposome (ΔH) was determined as well as a binding constant, K_a, reflecting the affinity of the lipopeptide for the liposomes and the stoichiometry of the binding, n, that is the number of phospholipids per peptide (Table 2). As seen, the binding of C_{16}–KK–NH_2 (**I**) and C_{16}–KGK–NH_2 (**II**) to POPG vesicles is an enthalpy-driven exothermic reaction (Fig. 3). The apparent association constant of the latter with the POPG membrane decreases almost three times in comparison to the former indicating that a neutral amino acid inserted between the positively charged lysine residues affects evidently the binding affinity of the peptide to the negatively charged membrane. This finding is in good agreement with the previous studies of peptides composed of basic residues [22]. In the case of C_{16}–KKKK–NH_2 (**III**), association with the negatively charged POPG membrane occurs with no detectable enthalpy changes under experimental conditions and only the small, constant, and exothermic heat flows suggest a weak or no interaction between the peptide and the lipid bilayer. This is all the more surprising because previous studies with Lys_n (n = 2–5) have shown that each Lys added to dilysine increased by one order of magnitude the binding affinity of the peptide for negatively charged membranes [22]. Hence, one can expect that analog **III** should exhibit a higher affinity for the POPG membrane than analog **I**. Similar discrepancies have been reported by Montich et al. [23]. Titration of Lys_5 to anionic POPG lipids produced only small endothermic binding enthalpy, which dropped to 0 kcal/mol upon binding of Lys_5 to the large unilamellar vesicle. This finding pointed to the entropy-driven binding process that also depends on vesicle size. Blume and co-workers [24] have highlighted that the side chains of basic amino acids such as lysine not only provide a positive charge, but also a flexible hydrocarbon spacer that enables hydrophobic interactions. Hence, the binding of Lys_5 to POPG vesicles is a resultant action of compensating contributions from both electrostatic and hydrophobic interactions. In our opinion, such a compensation of both interactions appears in C_{16}–KKKK–NH_2 (**III**). Moreover, it is proposed that an increase in endothermic contribution due to hydrophobic interactions is the result of desolvation of both the peptide and the membrane surface during interactions. As a matter of fact, electrostatic attraction drives the positively charged peptide toward the surface of the negatively charged membrane, but as the peptide approaches the membrane, the repulsive desolvation force becomes greater than the attractive electrostatic one. This results in a significant increase in favorable hydrophobic interactions mediated by non-polar fragments of the peptide, leading to incorporation of the peptide into membrane core [25,26].

In the case of all the peptides studied, each injection of the zwitterionic POPC lipids into the reaction cell containing lipopeptide produced an endothermic heat of reaction which decreased only slightly in magnitude with subsequent injections and remained incomplete even after 46 lipid injections (Fig. 4). Thus, the titration does not provide the total binding enthalpy indicating only very weak interactions.

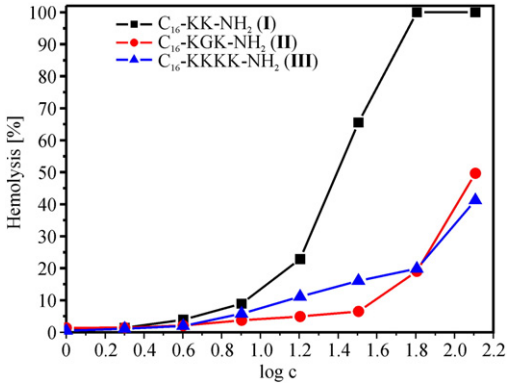

Fig. 2. Hemolytic activities of lipopeptide compounds: C_{16}–KK–NH_2 (**I**), C_{16}–KGK–NH_2 (**II**) and C_{16}–KKKK–NH_2 (**III**). The concentrations are given in μg/mL and presented as log c.

3.3. FT-IR spectroscopy: effects of lipopeptide binding on lipid organization

The frequencies of the asymmetric $\nu_{as}(CH_2)$ and symmetric $\nu_s(CH_2)$ stretching bands of the methylene groups belonging to the acyl chains of the phospholipids are adequate indicators of the phase transition from the gel phase ($L_{\beta'}$) to the liquid crystalline (L_α) phase. It is known that the "melting" of the all-*trans* chains of the phospholipids in the gel phase to the liquid-crystalline one increases the number of *gauche* conformers. At the main phase transition point, the bilayer model contains equal percentages of the ordered and disordered phospholipids. The phase transition points are dependent on the chemical nature of the model membrane constituents [27,28].

The lipids undergo a highly cooperative chain melting phase transition, as indicated by an abrupt increase in the $\nu_{as}(CH_2)$ and $\nu_s(CH_2)$ frequencies from the values around 2917 cm^{-1} and 2850 cm^{-1} at the temperature below the transition point up to around 2923 cm^{-1} and

Table 2
Thermodynamic parameters for lipopeptides binding to the LUVs POPG vesicle.

Lipopeptide	n	K_a 10^5 mol^{-1}	ΔH kcal/mol	ΔG kcal/mol	ΔS cal/mol/deg
C_{16}–KK–NH_2	1.4	9.06	−0.34	−10.05	34.09
C_{16}–KGK–NH_2	1.7	3.04	−0.58	−9.85	31.10

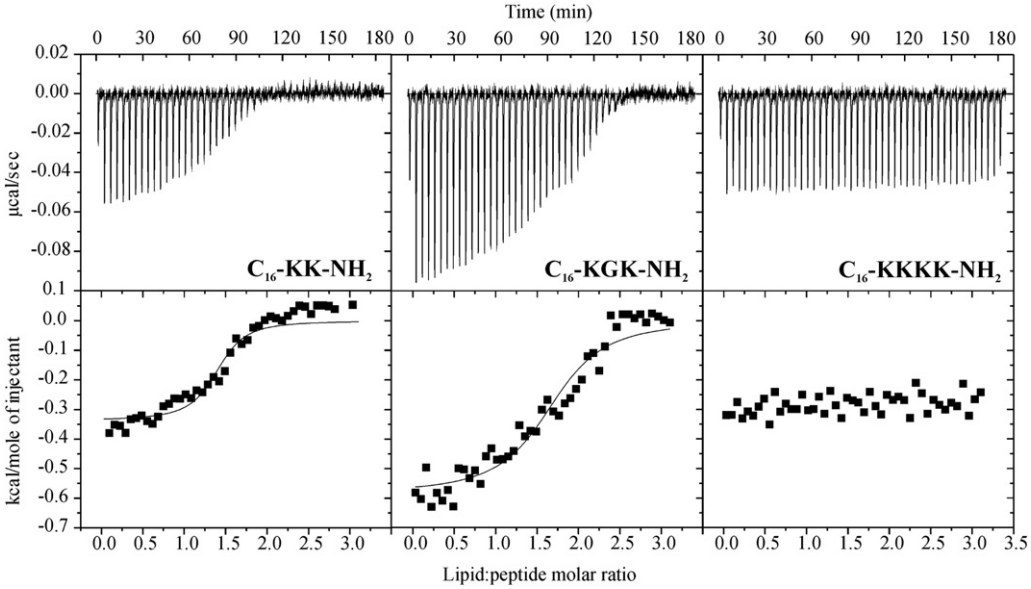

Fig. 3. Isothermal titration of lipopeptides with POPG LUVs at 25 °C. The lower curves represent the heat of reaction (measured by peak integration) as a function of the lipid/peptide molar ratio.

2853 cm^{-1} for asymmetric and symmetric stretching vibrations, respectively, at a higher temperature. Fig. 5 displays an evolution of the maximum frequency of the $\nu_s(CH_2)$ as a function of temperature for DPPC and DPPG, in the absence and in the presence of the lipopeptides. The first derivative of the curve was calculated to detect more precisely the T_m of the lipids and lipid–peptide mixtures. The lipid:peptide molar ratio was 10:1. In addition, in the case of the DPPG:C_{16}–KKKK–NH_2 (**III**) system, the FT-IR spectra were also taken for the sample with the 4:1 molar ratio.

As seen in Fig. 5, the lipopeptides show a significant influence on the hydrophobic core region of the DPPC membrane. The T_m of DPPC decreases by 0.8–2.1 °C upon premixing with the lipopeptides studied. A lower phase transition temperature means that the arrangement of the lipid matrix is perturbed, which is the consequence of a close contact of the lipopeptides with the hydrophobic part of the membrane. Besides, the peak positions of the stretching band remain significantly above those of the pure DPPC in both the gel and fluid phases indicating an increase in membrane fluidity within the entire temperature range. In turn, addition of the lipopeptides to anionic lipid DPPG vesicles results in diverse influence on the DPPG phase behavior. In the case of C_{16}–KK–NH_2 (**I**), only a slight increase in the phase transition temperature is observed (Fig. 5). However, introduction of a neutral Gly residue between two positively charged lysines dramatically changed interactions with the DPPG vesicles. Hence, in the case of

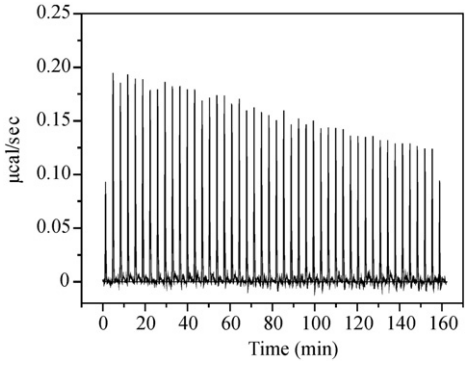

Fig. 4. Isothermal titration of C_{16}–KKKK–NH_2 (**III**) with POPC LUVs at 25 °C. Each injection produces an endothermic heat of reaction which decreased only slightly in magnitude with subsequent injections. The binding appears to remain incomplete even after 46 lipid injections.

C_{16}–KGK–NH_2 (**II**), T_m dropped by about 1.5 °C. Still more interesting results have been found for C_{16}–KKKK–NH_2 (**III**). This compound has the highest overall positive charge among the peptides studied. However, contrary to expectations, it has no marked influence on the behavior of the DPPG phase, even upon increasing its concentration up to the DPPG:peptide molar ratio of 4:1, where the total charge compensation occurs (Fig. 5). It is believed that the effective screening of the negatively charged DPPG head groups upon electrostatic binding of the positively charged molecule reduces the lateral repulsions between the lipids and consequently the gel phase is stabilized, as manifested by shifting the transition toward a higher temperature [29]. In turn, a partial insertion of the molecule into the membrane driven by hydrophobic interactions induces fluidization of the bilayer and deformation of the packing of the phospholipid acyl chain typically leads to a decrease in the transition temperature [24,30]. In our opinion, in the case of C_{16}–KKKK–NH_2 (**III**), compensation of hydrophobic and electrostatic interactions leads to almost no overall effect on T_m. However, raising the C_{16}–KKKK–NH_2 (**III**) concentration results in a distinct decrease in $\nu_s(CH_2)$ wavenumber below the T_m, which is typically related to an increase of the lipid acyl chain ordering. On the other hand, the increase of the lipid acyl chain ordering in the gel phase should lead to a distinct increase in T_m, which is inconsistent with our data. Thus, the decrease in the wavenumber is rather due to an increase in interchain vibrational coupling caused by a reduction of rotational disorder of the chains after peptide **III** binding [29,31].

3.4. Critical micellar concentration increases with steric hindrance and electrostatic repulsion

Due to the surfactant-like structure of the lipopeptides, their critical micellar concentrations (CMCs) were determined using the surface tension measurements versus log of the lipopeptide concentration. CMCs of C_{16}–KK–NH_2 (**I**), C_{16}–KGK–NH_2 (**II**) and C_{16}–KKKK–NH_2 (**III**) were estimated to be 1.07 mM (547 μg/mL), 1.89 mM (1,070 μg/mL) and 14.6 mM (11,200 μg/mL), respectively. It is known, that the micellization process in aqueous solution results from a balance of different intermolecular forces, including hydrophobic, steric, electrostatic, hydrogen bonding and van der Waals interactions. Nevertheless, the driving force for sell-assembly of surfactant molecules in aqueous solution is the hydrophobic effect. An increase in hydrophobicity of a surfactant reduces the CMC. Hence, the CMC decreases with increasing hydrocarbon chain length and decreasing the size of the head group

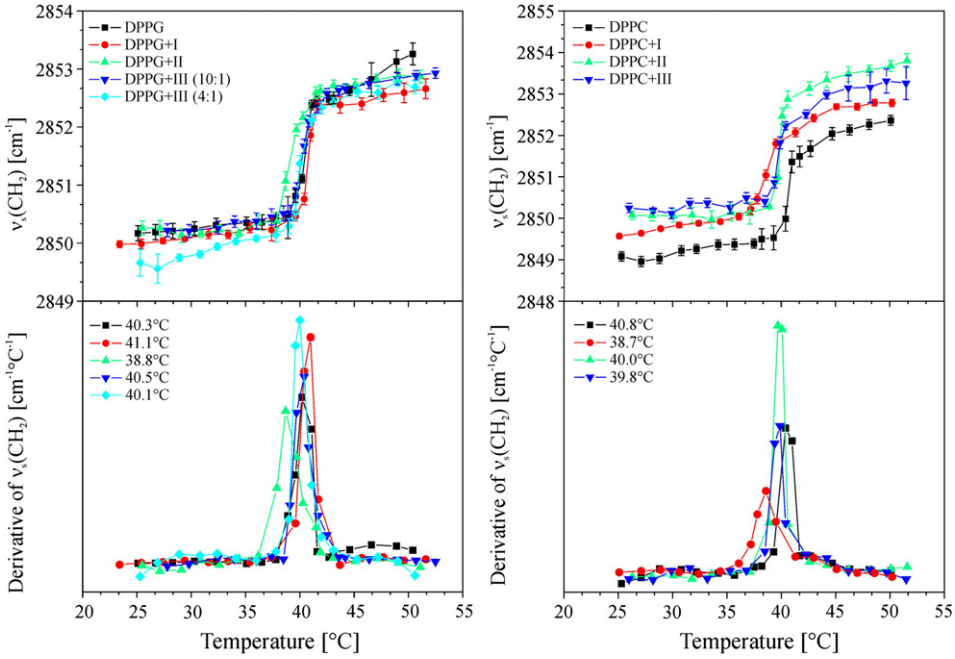

Fig. 5. Evolution of the maximum frequency of the $\nu_s(CH_2)$ stretching vibrations as a function of temperature and their first derivatives for DPPC and DPPG in the absence and in the presence of the peptide. The peak maxima in the bottom panels indicate the transition temperature. The concentration of phospholipids was 50 mg/mL.

[32–34]. Due to the fact that all the peptides studied have the same hydrocarbon chain length, any changes of CMC value are determined by polar head groups. Our results show that the CMC value increases when the polar head group becomes bigger. With C_{16}–KGK–NH_2 (**II**), introduction of a neutral glycine residue affected the size of the polar head group but not the overall charge as compared to that of C_{16}–KK–NH_2 (**I**). Consequently, steric interactions seem to be a major factor opposing micelle formation reflected in the slight increase of CMC. In turn, in the case of C_{16}–KKKK–NH_2 (**III**), high CMC value is the consequence of an increase in the size and in charge of the polar head group. This compound has twice as high total positive charge as the two remaining ones, which modifies balance between hydrophilic and hydrophobic properties. As seen in the example of C_{16}–KKKK–NH_2 (**III**), an increase in the hydrophilicity of the lipopeptide increases the CMC, the finding being compatible with the literature data [35].

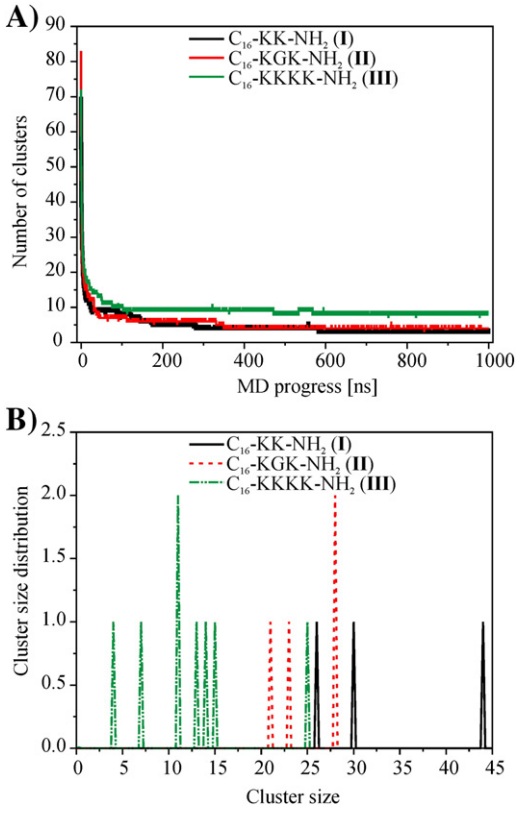

Fig. 6. (A) Number of clusters as a function of time and (B) cluster size distributions over the last 100 ns of CG MD simulations.

3.5. Coarse-grained molecular dynamics: self-organization of lipopeptides

In Fig. 6, the aggregation process is presented as a function of time for each lipopeptide. Two detergent molecules were classified into the same cluster if any of their alkyl chain beads fell within the distance of 6 Å of each other. The self-assembly can be considered as a three-step process, i.e. a quick aggregation of the monomers into small clusters, fusion of these clusters into larger ones and formation of micelles. In the last step, the aggregation process reaches an equilibrium and the micelles do not aggregate further even when their hydrophilic shells come into contact. This is due to the repulsion between positively charged Lys residues being unfavorable for micellization. The number of clusters appears to stabilize at ca. 600 ns and remains at a constant level up to the end of simulation. Fig. 6B displays the cluster size distributions calculated for each system in the last 100 ns of CG MD simulations. As seen, the size and charge of the head group are major determinants for the micelle aggregation number. The trend observed shows that with an increase in size of the head group the aggregation number decreases, which is compatible with the literature data [36]. In the case of peptide **III**, an increase in the overall charge of the monomer results in a stronger electrostatic repulsion, which additionally reduces the aggregation number. In ca. 90% of the micelle of this peptide, the aggregation number does not exceed 15. Perhaps not all the lysine residues are protonated upon micelle formation. In this situation, the size of the clusters should be bigger.

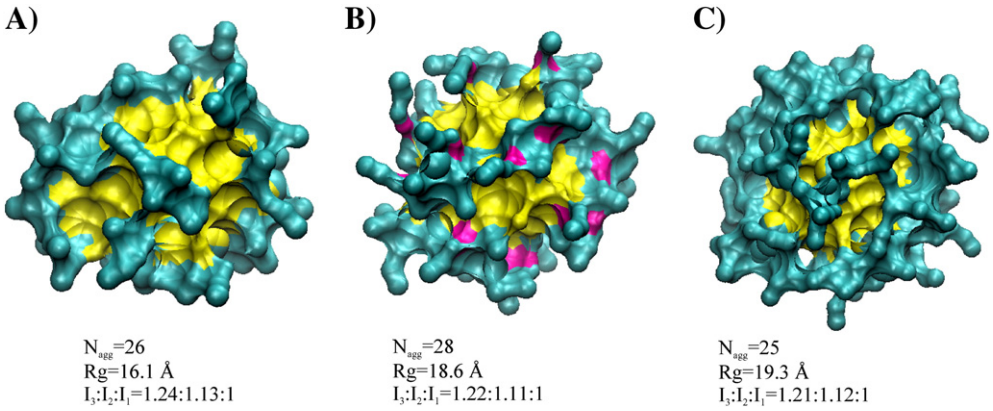

Fig. 7. Individual micelles from final snapshots of CG MD simulations with similar aggregation numbers: (A) C_{16}–KK–NH_2 (**I**), (B) C_{16}–KGK–NH_2 (**II**) and (C) C_{16}–KKKK–NH_2 (**III**). Fatty acid tails are colored yellow, while lysines and glycines from head groups are colored cyan and magenta, respectively. Aggregation numbers, radii of gyration, and ratios of moments of inertia are given beneath each picture.

To compare the micelles formed by different lipopeptides, we selected those with similar aggregation number (Fig. 7). Hence, for peptides **II** and **III**, the micelle with the highest aggregation number, and peptide **I**, the micelle with the lowest aggregation number in the entire system have been chosen for further analysis. The average radii of gyration (R_g) of the micelles over the last 100 ns of simulations are 16.1, 18.8 and 19.3 Å for peptides **I**, **II** and **III**, respectively. Thus, the effective radii of the micelles, based on the relationship between the radius of a solid sphere of uniform density and its radius of gyration [37], should be about 20.8, 24.3 and 24.9 Å, respectively. An analysis of the micelles' shape by calculating the ratio of the average principal moments of inertia tensors (Table 1S, Supplementary material) indicates a deviation from the spherical shape. The average moments of inertia for the C_{16}–KK–NH_2 (**I**), C_{16}–KGK–NH_2 (**II**) and C_{16}–KKKK–NH_2 (**III**) micelles over the last 100 ns of simulations are in the ratios of 1.24:1.13:1, 1.22:1.11:1 and 1.21:1.12:1, respectively, revealing a prolate shape of the aggregates.

Fig. 1S (Supplementary material) shows the density profiles of various groups in the selected micelles as a function of the distance from micelle's mass center (COM). As expected, the hydrophobic interior of the micelles is devoid of solvent molecules and chloride ions. The distribution of water does not extend much at a distance of ca. 10 Å from COM. Penetration of chloride ions into the micelles is less than that of water and, regardless of the size of the monomer's head group, the density of the ions reaches a maximum value of ca. 20 Å. The fluidity of the hydrocarbon chain in the lipopeptide micelles can be assessed by probability distribution function of various hydrocarbon beads with respect to the micelle COM (Fig. 2S, Supplementary material). The width of the C4 distribution oscillating around 18 Å in each case is visibly broader than for the other beads. This wide-spread distribution indicates that the terminal carbon atoms show the tendency to be turned toward the water/head group interface region rather than to be pointed to the COM in a straight line. The overall probability distributions of the beads from the head groups span the regions of 15 Å, 18 Å and 20 Å for C_{16}–KK–NH_2 (**I**), C_{16}–KGK–NH_2 (**II**) and C_{16}–KKKK–NH_2 (**III**), respectively. As seen, the addition of one residue to the polar head extends the distribution by 2–3 Å.

To evaluate the extent of torsional motion of the micelle, the angle formed by the vector between C1 and C4 sites and between C1 and the mass center of the micelle (C4–C1–COM) was examined (Fig. 3S, Supplementary material). The angle distribution mode is asymmetric and shifted toward the lower angle values. The nonzero angle values support the suggestion that the fatty acid chains are not perfectly aligned through the micelle COM. The fairly broad plateau observed in the range of 21° to 45° for peptides **I** and **III** is slightly shifted toward higher angle values for peptide **II** (24°–51°), indicating a somewhat different arrangement of lipid tails in micelle's interior. Besides, the average hydrophobic solvent accessible surface area (SASA) per molecule estimated to be 226 $Å^2$ for peptide **II** is lower by 8–13 $Å^2$

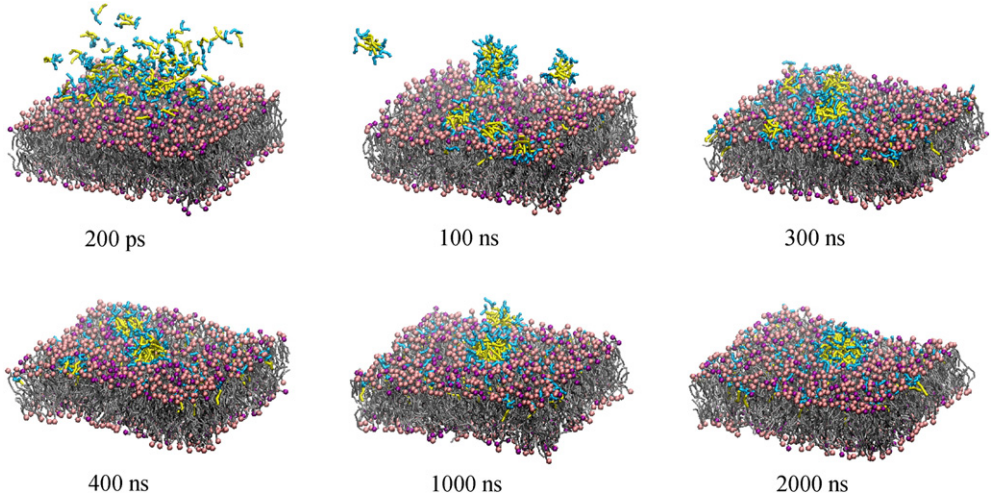

Fig. 8. Snapshots from the POPE:POPG binding simulations for C_{16}–KK–NH_2 (**I**). Fatty acid tails are colored yellow, while lysines are colored cyan. Lipid tails are colored gray, while lipid head groups are colored pink and purple for POPG and POPE, respectively.

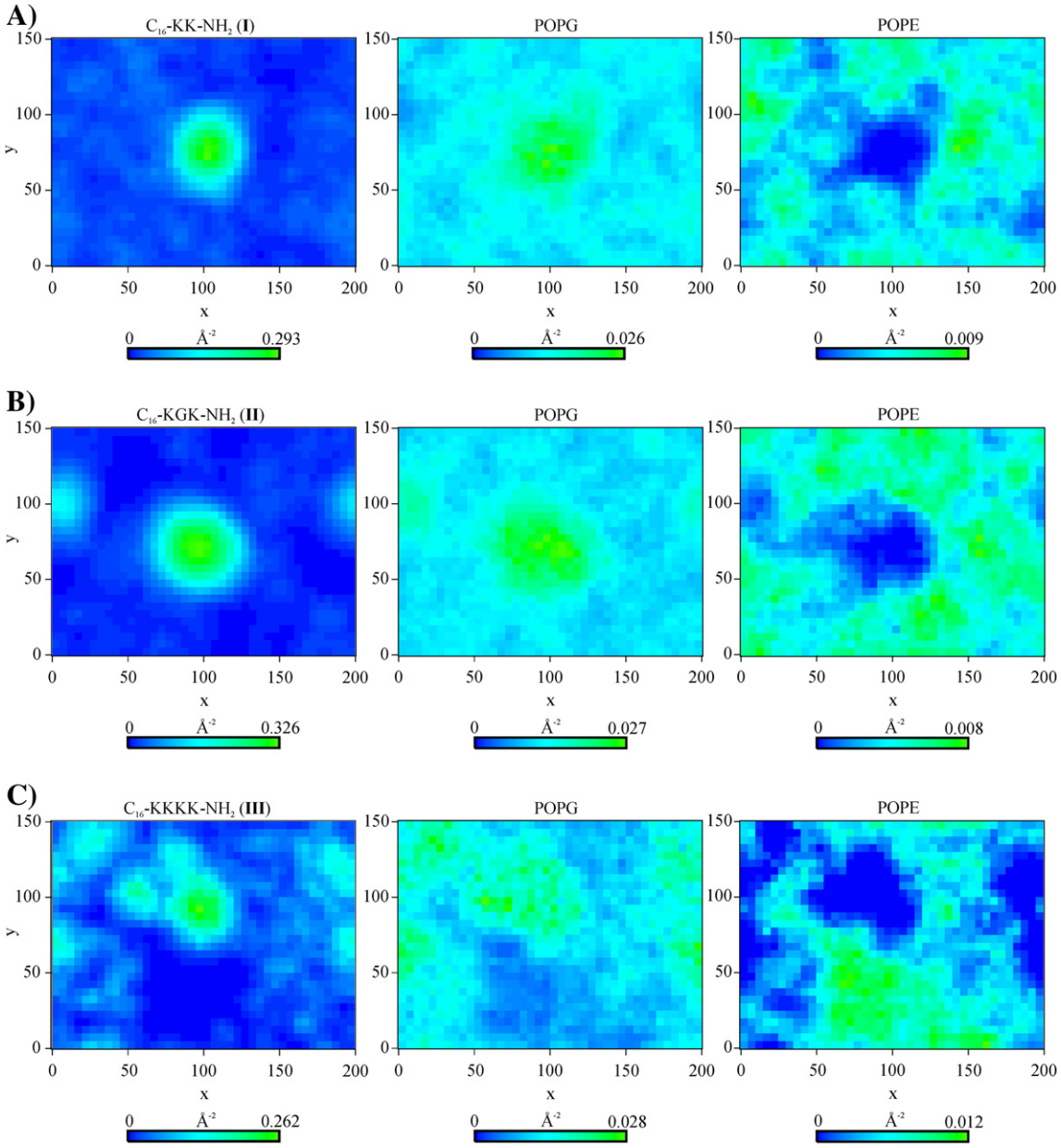

Fig. 9. 2D density map of the lipopeptides, POPG and POPE lipids in the upper leaflet of the membrane based on the last 100 ns of a total of 2 μs CG MD simulations. A grid spacing was set to 5 Å.

from that for the remaining peptides (Table 2S, Supplementary material), confirming a slightly different arrangement of the molecules relative to each other.

3.6. Coarse-grained molecular dynamics: lipopeptides bind and insert into the lipid bilayer

Coarse-grained molecular dynamics simulations were performed to visualize the binding and insertion of the lipopeptides into the bacterial membrane. In the first approach, the systems were built according to the procedure proposed by Horn et al. [38]. A representative micelle of each lipopeptide extracted in the first stage of the CG MD simulations (vide supra) was positioned on one leaflet of the lipid bilayer composed of POPE and POPG at a molar ratio of 1:3. For each lipopeptide, three unique systems were created, which differ from each other with initial distance between the micelle and the lipid bilayer. The systems were neutralized, minimized and subjected to NPT molecular dynamics simulations for 1 μs. However, despite many attempts, none of the micelles have been inserted into the membrane during the simulations as was reported for C_{16}–KGGk [38]. In each case, the micelle bound to the surface of the membrane and remained intact to the end of the CG MD simulations.

In the next step of our theoretical studies, other simulation systems were built in such a way that 100 molecules of each lipopeptide were randomly placed close to one leaflet of the 1:3 POPE:POPG lipid bilayer. In this approach, during the first nanosecond of simulations two concurrent processes were observed, i.e. association and incorporation of the monomers of the lipopeptides into the membrane and the self-organization of the lipopeptides into micelles. In the further stages of MD simulations, positively charged lipopeptide micelles are attracted by a negatively charged membrane surface. However, in the case of C_{16}–KGK–NH_2 (**II**) and C_{16}–KKKK–NH_2 (**III**), not all lipopeptide molecules clustered into aggregates were bound to one membrane leaflet and due to the periodic boundary conditions they were free to bind with the opposite leaflet of the lipid bilayer. This is probably a consequence of significant crowding of the lipopeptides in the initial state of simulations. Thus, to mimic the physiological conditions, where all the lipopeptides bind to the

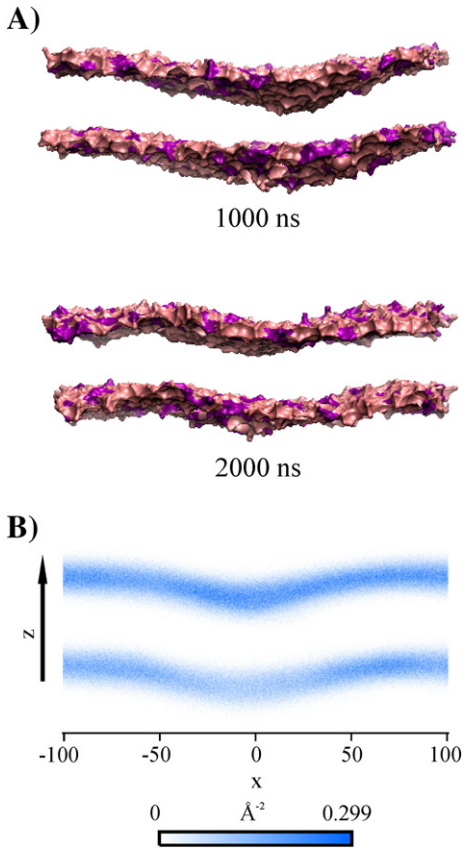

Fig. 10. (A) Membrane curvature induced by C_{16}–KGK–NH_2 (**II**) after 1 μs and 2 μs of CG MD simulations. Lipid head groups are colored pink and purple for POPG and POPE, respectively. (B) 2D density map of the lipid head groups in the upper and inner leaflets of the membrane based on the last 100 ns of a total of 2 μs CG MD simulations. A grid spacing was set to 1 Å.

outer leaflet of the lipid bilayer, the lipopeptide molecules not associated with the outer membrane surface were removed from the systems before they had been able to bind to the inner leaflet of the membrane. Afterwards, the systems were neutralized by addition of sodium ions, minimized and subjected to further NTP simulations. Consequently, the number of lipopeptide molecules in the systems with lipid bilayer decreased to 97 and 87 for C_{16}–KGK–NH_2 (**II**) and C_{16}–KKKK–NH_2 (**III**), respectively.

In subsequent steps of the CG MD simulations, small surface-bound aggregates of the lipopeptides either insert into the lipid bilayer and upon complete insertion the lipopeptide molecules are gradually dispersed or move toward each other and fuse to form larger micelles still associated with the membrane surface. Fig. 8 displays snapshots from the POPE:POPG binding simulations for C_{16}–KK–NH_2 (**I**). The snapshots from simulations for two remaining systems are shown in Figs. 4S and 5S (Supplementary material). As seen, not all surface-bound micelles were inserted into the lipid bilayer during the simulations. Nevertheless, these micelles affect the membrane structure through a distinct enrichment of POPG lipids at the binding site with membrane surface resulting in some POPG-rich domains (Fig. 9) and by modulation of the membrane curvature (Fig. 10).

4. Conclusion

In recent years, there has been an increased interest in application of short cationic lipopeptides as a group of compounds with promising antimicrobial properties. Previous studies have shown that conjugation of aliphatic fatty acid with the *N*-terminus of peptides affects both their antimicrobial potency and physicochemical properties [39]. Avrahami and Shai [40] reported that the presence of a hydrocarbon chain increases the hydrophobicity of the peptides and their self-assembling capacity in solution, which translates into interactions with the biological membrane of microorganisms.

In the current paper, we present the results of studies on three short synthetic cationic lipopeptides modified with palmitic acid. All the lipopeptides presented in this paper show surface-active properties with clear CMC in the millimolar range (1.07–14.6 mM). An increase of steric and electrostatic repulsion between polar head groups shifts the CMC to higher values and reduces the aggregation number. It should be emphasized that achieving critical micellar concentration is not necessary for inducing antimicrobial activity and all the peptides studied inhibited microbial growth at concentrations below that required for micelle formation.

Previous theoretical studies on the mechanism of action of the short cationic antimicrobial lipopeptide, C_{16}–KGGk, have shown that the compound prefers to aggregate in solution and changes the inner ordering of the lipid bilayer upon binding. In the fully inserted state, the acyl chains are completely buried in the hydrophobic core of the membrane, while the peptide fragment remains largely hydrated and is in close contact with the head groups [38,41]. In our work, the binding of the lipopeptides to anionic lipids has been found to be a process consisting of a balance between electrostatic and hydrophobic interactions. The substantial compensation of electrostatic and hydrophobic interactions is clearly evident in the case of C_{16}–KKKK–NH_2 (**III**), where no overall effects of binding to monovalent anionic lipids were noticed on ITC thermograms and FTIR spectra. However, the presence of the fatty acid chain enables penetration into zwitterionic vesicle, which is reflected in the reduction of the main transition point of the lipid and in increasing membrane fluidity. In the case of each lipopeptide, the binding to zwitterionic vesicle is entropy-driven and is too weak to be precisely quantified by the ITC method. Nevertheless, the interactions of the lipopeptides with pure zwitterionic phospholipids provide a clear picture of the role of hydrophobic interactions in lipopeptide–membrane binding process. In our opinion, a unique interplay between the initial electrostatic and subsequent hydrophobic interactions confers lipopeptides the ability to interact with the lipid bilayer. The palmitic acid tail may penetrate into the hydrophobic core of the membrane, whereas the basic Lys residues contribute to membrane association through favorable electrostatic interactions with anionic lipids. Both types of interactions provide a sufficient energy to anchor the peptide into the membrane.

Acknowledgements

This work was supported by the University of Gdańsk (DS. 530-8453-D381-13). We are grateful to Dr. Dariusz Wyrzykowski (University of Gdańsk) for his technical assistance in ITC measurements.

Appendix A. Supplementary data

Supplementary data to this article can be found online at http://dx.doi.org/10.1016/j.bbamem.2014.06.016.

References

[1] R.E. Hancock, H.-G. Sahl, Antimicrobial and host-defense peptides as new anti-infective therapeutic strategies, Nat. Biotechnol. 24 (2006) 1551–1557.
[2] A.E. Bilsland, C.J. Cairney, W. Nicol Keith, Targeting the telomere and shelterin complex for cancer therapy: current views and future perspectives, J. Cell. Mol. Med. 15 (2011) 179–186.
[3] M.N. Melo, R. Ferre, M.A. Castanho, Antimicrobial peptides: linking partition, activity and high membrane-bound concentrations, Nat. Rev. Microbiol. 7 (2009) 245–250.
[4] K. Hall, H. Mozsolits, M.-I. Aguilar, Surface plasmon resonance analysis of antimicrobial peptide–membrane interactions: affinity & mechanism of action, Lett. Pept. Sci. 10 (2003) 475–485.
[5] L.M. Rossi, P. Rangasamy, J. Zhang, X.Q. Qiu, G.Y. Wu, Research advances in the development of peptide antibiotics, J. Pharm. Sci. 97 (2008) 1060–1070.

[6] W.C. Wimley, Describing the mechanism of antimicrobial peptide action with the interfacial activity model, ACS Chem. Biol. 5 (2010) 905–917.
[7] B.M. Peters, M.E. Shirtliff, M.A. Jabra-Rizk, Antimicrobial peptides: primeval molecules or future drugs? PLoS Pathog. 6 (2010) e1001067.
[8] A. Giuliani, G. Pirri, S.F. Nicoletto, Antimicrobial peptides: an overview of a promising class of therapeutics, Cent. Eur. J. Biol. 2 (2007) 1–33.
[9] Y.J. Gordon, E.G. Romanowski, A.M. McDermott, A review of antimicrobial peptides and their therapeutic potential as anti-infective drugs, Curr. Eye Res. 30 (2005) 505–515.
[10] M. Dawgul, W. Baranska-Rybak, E. Kamysz, A. Karafova, R. Nowicki, W. Kamysz, Activity of short lipopeptides and conventional antimicrobials against planktonic cells and biofilms formed by clinical strains of *Staphylococcus aureus*, Futur. Med. Chem. 4 (2012) 1541–1551.
[11] A. Makovitzki, A. Viterbo, Y. Brotman, I. Chet, Y. Shai, Inhibition of fungal and bacterial plant pathogens in vitro and in planta with ultrashort cationic lipopeptides, Appl. Environ. Microbiol. 73 (2007) 6629–6636.
[12] M. Dawgul, W. Barańska-Rybak, K. Greber, Ł. Guzik, R. Nowicki, J. Łukasiak, W. Kamysz, Aktywność przeciwbakteryjna krótkich lipopeptydów wobec klinicznych szczepów *Staphylococcus aureus*, Alerg. Astma Immunol. 16 (2011) 31–36.
[13] O. Cirioni, A. Giacometti, R. Ghiselli, W. Kamysz, C. Silvestri, F. Orlando, F. Mocchegiani, A.D. Vittoria, E. Kamysz, V. Saba, G. Scalise, The lipopeptides Pal-Lys-Lys-NH(2) and Pal-Lys-Lys soaking alone and in combination with intraperitoneal vancomycin prevent vascular graft biofilm in a subcutaneous rat pouch model of staphylococcal infection, Peptides 28 (2007) 1299–1303.
[14] G.B. Fields, R.L. Noble, Solid-phase peptide-synthesis utilizing 9-fluorenylmethoxycarbonyl amino-acids, Int. J. Pept. Protein Res. 35 (1990) 161–214.
[15] P. Garidel, C. Johann, L. Mennicke, A. Blume, The mixing behavior of pseudobinary phosphatidylcholine phosphatidylglycerol mixtures as a function of pH and chain length, Eur. Biophys. J. Biophys. Lett. 26 (1997) 447–459.
[16] U. Kim, Y.S. Kim, S. Han, Modulation of cytochrome c-membrane interaction by the physical state of the membrane and the redox state of cytochrome c, Bull. Kor. Chem. Soc. 21 (2000) 412–418.
[17] B. Hess, C. Kutzner, D. Van Der Spoel, E. Lindahl, GROMACS 4: algorithms for highly efficient, load-balanced, and scalable molecular simulation, J. Chem. Theory Comput. 4 (2008) 435–447.
[18] X. Periole, S.J. Marrink, The MARTINI coarse-grained force field, Methods Mol. Biol. 924 (2013) 533–565.
[19] S.J. Marrink, H.J. Risselada, S. Yefimov, D.P. Tieleman, A.H. de Vries, The MARTINI force field: coarse grained model for biomolecular simulations, J. Phys. Chem. B 111 (2007) 7812–7824.
[20] M. Winger, D. Trzesniak, R. Baron, W.F. van Gunsteren, On using a too large integration time step in molecular dynamics simulations of coarse-grained molecular models, Phys. Chem. Chem. Phys. 11 (2009) 1934–1941.
[21] A. Chugunov, D. Pyrkova, D. Nolde, A. Polyansky, V. Pentkovsky, R. Efremov, Lipid-II forms potential "landing terrain" for lantibiotics in simulated bacterial membrane, Sci. Rep. 3 (2013), http://dx.doi.org/10.1038/srep01678.
[22] J. Kim, M. Mosior, L.A. Chung, H. Wu, S. McLaughlin, Binding of peptides with basic residues to membranes containing acidic phospholipids, Biophys. J. 60 (1991) 135–148.
[23] G. Montich, S. Scarlata, S. McLaughlin, R. Lehrmann, J. Seelig, Thermodynamic characterization of the association of small basic peptides with membranes containing acidic lipids, Biochim. Biophys. Acta Biomembr. 1146 (1993) 17–24.
[24] M. Hoernke, C. Schwieger, A. Kerth, A. Blume, Binding of cationic pentapeptides with modified side chain lengths to negatively charged lipid membranes: complex interplay of electrostatic and hydrophobic interactions, Biochim. Biophys. Acta Biomembr. 1818 (2012) 1663–1672.
[25] S.A. Simon, T.J. McIntosh, Peptide–Lipid Interactions, Vol. 52Academic Press, 2002.
[26] T. Abraham, R.N. Lewis, R.S. Hodges, R.N. McElhaney, Isothermal titration calorimetry studies of the binding of the antimicrobial peptide gramicidin S to phospholipid bilayer membranes, Biochemistry 44 (2005) 11279–11285.
[27] F. Severcan, D.-O. Dorohoi, FTIR studies of temperature influence on the DPPG model membrane, J. Mol. Struct. 887 (2008) 117–121.
[28] H. Bensikaddour, K. Snoussi, L. Lins, F. Van Bambeke, P.M. Tulkens, R. Brasseur, E. Goormaghtigh, M.-P. Mingeot-Leclercq, Interactions of ciprofloxacin with DPPC and DPPG: fluorescence anisotropy, ATR-FTIR and (31)P NMR spectroscopies and conformational analysis, Biochim. Biophys. Acta Biomembr. 1778 (2008) 2535–2543.
[29] C. Schwieger, A. Blume, Interaction of poly(L-lysines) with negatively charged membranes: an FT-IR and DSC study, Eur. Biophys. J. Biophys. Lett. 36 (2007) 437–450.
[30] D. Papahadjopoulos, M. Moscarello, E. Eylar, T. Isac, Effects of proteins on the thermotropic phase transitions of phospholipid membranes, Biochim. Biophys. Acta Biomembr. 401 (1975) 317–335.
[31] A. Arouri, M. Dathe, A. Blume, Peptide induced demixing in PG/PE lipid mixtures: a mechanism for the specificity of antimicrobial peptides towards bacterial membranes? Biochim. Biophys. Acta Biomembr. 1788 (2009) 650–659.
[32] C.O. Rangel-Yagui, A. Pessoa Jr., L.C. Tavares, Micellar solubilization of drugs, J. Pharm. Pharm. Sci. 8 (2005) 147–163.
[33] K. Meguro, M. Ueno, K. Esumi, Micelle formation in aqueous media, Nonionic Surfactants: Physical Chemistry, 1987. 109–183.
[34] A. Dominguez, A. Fernandez, N. Gonzalez, E. Iglesias, L. Montenegro, Determination of critical micelle concentration of some surfactants by three techniques, J. Chem. Educ. 74 (1997) 1227.
[35] E. Mahmood, D.A. Al-Koofee, Effect of temperature changes on critical micelle concentration for tween series surfactant, Global J. Sci. Front. Res. 13 (2013).
[36] R.C. Oliver, J. Lipfert, D.A. Fox, R.H. Lo, S. Doniach, L. Columbus, Dependence of micelle size and shape on detergent alkyl chain length and head group, PLoS ONE 8 (2013) e62488.
[37] S. Bogusz, R.M. Venable, R.W. Pastor, Molecular dynamics simulations of octyl glucoside micelles: structural properties, J. Phys. Chem. B 104 (2000) 5462–5470.
[38] J.N. Horn, J.D. Sengillo, D. Lin, T.D. Romo, A. Grossfield, Characterization of a potent antimicrobial lipopeptide via coarse-grained molecular dynamics, Biochim. Biophys. Acta Biomembr. 1818 (2012) 212–218.
[39] A. Malina, Y. Shai, Conjugation of fatty acids with different lengths modulates the antibacterial and antifungal activity of a cationic biologically inactive peptide, Biochem. J. 390 (2005) 695–702.
[40] D. Avrahami, Y. Shai, A new group of antifungal and antibacterial lipopeptides derived from non-membrane active peptides conjugated to palmitic acid, J. Biol. Chem. 279 (2004) 12277–12285.
[41] J.N. Horn, T.D. Romo, A. Grossfield, Simulating the mechanism of antimicrobial lipopeptides with all-atom molecular dynamics, Biochemistry 52 (2013) 5604–5610.